Transport processes in a combustible turbulent boundary layer

By NORMAN G. KULGEIN
Lockheed Missiles and Space Company, Sunnyvale, California

(Received 21 July 1961)

Coexistent processes of heat, mass and momentum transfer operative within a combustible turbulent boundary layer have been experimentally investigated. The boundary layer was established on a porous cylinder mounted in a low-speed wind tunnel with its long axis in the flow direction. Methane was transpired into the boundary layer and ignited. Results indicate that the dimensionless transfer numbers corresponding to the three transfer processes can be correlated by the formula $0{\cdot}038Re^{-0{\cdot}2}$ to within $\pm 30\,\%$ of measured values so that a rough numerical analogy exists among all three processes. The effect of mass injection on the skin friction coefficient is reasonably well accounted for by available theory. No effect of mass injection was found on the values of heat and mass transfer parameters. Finally, there was a lack of evidence indicating any sort of reaction-generated turbulence or that the experimentally demonstrated disturbance of the viscous layer by mass injection substantially affected the transport phenomena.

1. Introduction

Three important transport processes that can occur simultaneously in fluid flows are heat, mass and momentum transfer. Indeed, these phenomena sometimes occur with the added complications of chemical reactions and phase changes. Some theoretical work has been accomplished for such flows as laminar boundary layers. However, in neither the laminar nor the turbulent case has there been any systematic experimental investigation. The present work describes an experimental investigation of the heat-, mass-, and momentum-transfer processes operative in a combustible turbulent boundary layer. Moreover, the fuel was injected through a porous wall into the boundary layer so that the potential effects of mass injection were present.

2. Apparatus

The experimental apparatus used is shown in figure 1*a*, plate 1. It consisted of a porous tube 36 in. long, 1·5 in. in diameter, with an average pore size of $10\,\mu$. This pore size was created by using a specially woven stainless-steel mesh† fabricated from 0·001 in.-thick N-155 stainless-steel wire.

Structural rigidity of the porous wall was assured by using two inner tubes of standard '60' mesh N-155 screen size for support. A rounded brass nose piece

† Manufactured by the Aircraft Porous Media Company, Glen Cove, Long Island.

$3\frac{3}{4}$ in. long was fitted to the upstream end of the tube. The interior of the apparatus consisted of a water-based heat exchanger together with appropriate plumbing for uniform emission of a gaseous fuel from the porous cylinder. The completed assembly was mounted in a $1\frac{1}{2}$ ft.-square low-speed wind tunnel with the longitudinal tube-axis in the flow direction. Technical-grade methane was metered into the porous tube and ignited when the main air flow was turned on. The two independent variables were free-stream air velocity and fuel flow rate. It is worth noting that no type of flame holder was ever used in any of the experimental runs, since the brass nose-porous cylinder combination was aerodynamically smooth. That stable combustion would be possible under these circumstances was determined in the course of the experiments. In a broad sense, of course, the entire porous tube assembly was itself a flameholder. Figure 1*a*, plate 1, shows the tube with the gas ignited. The flame was stable at a number of positions along the tube, as shown in figure 1*b*, plate 1. Data were taken only for conditions which resulted in a flame nearly coincident with the beginning of the porous screen.

3. Experimental measurements

Experimental measurements were made of the temperature, composition, and velocity profiles in the burning boundary layer using the following techniques.

(1) Temperature profiles were determined by traverses made with a chromel-alumel thermocouple coated with borax to avoid possible catalytic effects. Most of the combustion reactions occurred in a zone thin compared with the thickness of the boundary layer. Measured temperatures in the boundary layer were therefore much lower than customary adiabatic flame temperatures. Consequently, there were no structural or material difficulties with the thermocouple.

(2) Composition profiles were determined by traverses made with a small quartz tube having a 0·007 in. hole at one end. Gas samples were analysed with a mass spectrometer. The gas analysis was performed at room temperature so that only stable molecular species were reported present. The probe was designed so that its 0·007 in. orifice flared rapidly to the 3 mm internal tube diameter. This interior nozzle was designed to quench the reaction of gases at the time of their ingestion by the probe.

(3) Velocity profiles were determined by traverses made with a specially designed total impact tube. It consisted of four stainless steel hypodermic tubes, two of which were of equal size (0·014 in.) and fitted inside the others. The two larger tubes were concentric and carried cooling water in and out of the probe to within $\frac{3}{8}$ in. of the tip. The two small tubes constituted this tip. One tube was deformed into an oval shape of width 0·015 in. to serve as an impact tube. The other was closed at its end but had a small 0·014 in. hole drilled on a side facing in a direction perpendicular to the free stream direction. Two advantages accrue from employing a scheme wherein the static and dynamic tubes are extremely close in spatial position. First, the effect of free convection currents within the probe, induced by an ambient non-uniform temperature field, can be negated by subjecting *both* tubes to the same environmental conditions. Secondly, it was found experimentally that the effect of small local

unsteadiness upon micromanometer readings was minimized, apparently because the static reference was similarly disturbed. In order to determine wall shear stress this same instrument was used as a 'Stanton tube'. Details of this procedure may be found in Preston (1959) and will be discussed later.

4. Theoretical considerations

We want to exhibit some of the general results of the theory of reacting boundary-layer flows. By 'reacting' is meant that the gas consists of chemically transmutable species, some of which (products) are actively being formed from the others (reactants). Specific application will be made to the reaction system used in the present experimental work, that of the combustion of methane, $CH_4 + 2O_2 \rightarrow CO_2 + 2H_2O$. The appropriate turbulent boundary-layer equations are obtained by formally taking the time average of corresponding laminar terms together with usual order-of-magnitude estimates and can be written as:

equation of continuity:

$$\frac{\partial}{\partial x}(\overline{\rho}\overline{u}) + \frac{\partial}{\partial y}(\overline{\rho}\overline{v} + \overline{\rho' v'}) = 0; \tag{1}$$

equation of momentum:

$$\overline{\rho}\overline{u}\frac{\partial \overline{u}}{\partial x} + (\overline{\rho}\overline{v} + \overline{\rho' v'})\frac{\partial \overline{u}}{\partial y} = \frac{\partial}{\partial y}\left(\epsilon_v \frac{\partial \overline{u}}{\partial y}\right) - \frac{\partial p}{\partial x}; \tag{2}$$

equation of species continuity:

$$\overline{\rho}\overline{u}\frac{\partial \overline{Y}_i}{\partial x} + (\overline{\rho}\overline{v} + \overline{\rho' v'})\frac{\partial \overline{Y}_i}{\partial y} = \frac{\partial}{\partial y}\left(\overline{\rho}\epsilon_{d,i}\frac{\partial \overline{Y}_i}{\partial y}\right) + \overline{w}_i; \tag{3}$$

equation of energy:

$$\overline{\rho}\overline{u}\frac{\partial}{\partial x}(\overline{H} + \tfrac{1}{2}\overline{u}^2) + (\overline{\rho}\overline{v} + \overline{\rho' v'})\frac{\partial}{\partial y}(\overline{H} + \tfrac{1}{2}\overline{u}^2) = \frac{\partial}{\partial y}\left[\epsilon_\lambda \sum_i \frac{\partial}{\partial y}(\overline{h}_i \overline{Y}_i + \tfrac{1}{2}\overline{u}^2) + \sum_i \overline{\rho}\epsilon_{d,i}(1 - Le_T^{-1})\overline{h}_i \frac{\partial \overline{Y}_i}{\partial y} + \epsilon_v(1 - Pr_T^{-1})\frac{\partial}{\partial y}(\tfrac{1}{2}\overline{u}^2)\right]. \tag{4}$$

In this system of equations the ϵ_v, $\epsilon_{d,i}$, ϵ_λ are, respectively, the conductivities of momentum, mass, and thermal energy. In the turbulent part of the flow they are usually defined by the ratio of the Reynolds stresses, mass diffusivity or thermal diffusivity to the appropriate mean property gradient, e.g.

$$\epsilon_{d,i} \equiv \frac{-\overline{v' Y_i'}}{\partial \overline{Y}_i / \partial y}.$$

If there exists a 'viscous' region in the flow, these coefficients are to be interpreted as the more familiar 'molecular' coefficients, μ, $\mathscr{D}_{ij}$, λ. If there are regions where both turbulent and molecular transport processes are important then the coefficients are understood to reflect an appropriate combination of these effects. No more detailed information is required since only ratios among them are important. Furthermore, u and v are the velocity components in the x- and y-directions where x is measured along the surface and y is measured normal to it. The pressure is denoted by p, the density by ρ, the mass fraction of component i by Y_i, the volumetric mass rate of production of species i by w_i,

the Prandtl number by Pr_T, the Lewis number by Le_T, the total enthalpy by H. Bars over a quantity denote averaged values; primes denote fluctuating values.

Use of the species mass fraction in the continuity and energy equation as the 'driving force' for mass transfer warrants further discussion. It can be shown, using the kinetic theory of gases, that, for a binary mixture, the correct diffusion law is given by $\tilde{\rho}_i v_i = -\tilde{\rho}\mathscr{D}\,\mathrm{grad}\,X_i$ where $\tilde{\rho}_i v_i$ is the molar diffusive flux of component i relative to the mean *molar* flow, $\mathscr{D}$ is the diffusion coefficient and X_i is mole fraction. This form is equivalent to $\rho_i v_i = -\rho\mathscr{D}\,\mathrm{grad}\,Y_i$ where $\rho_i v_i$ is now to be taken as the diffusive *mass* flux of component i relative to the mean mass flow. These assertions can be verified by noting that the difference in flow velocities of the two species in either frame of reference must be the same. In terms of mole fractions, $(v_1 - v_2)_{\mathrm{diff}} = -(X_1 X_2)^{-1}\mathscr{D}\,\mathrm{grad}\,X_1$ so that the requirement for consistency is simply (noting that for a binary system $\mathscr{D}$ is not a function of composition) that $(X_1 X_2)^{-1}\nabla X_1 = (Y_1 Y_2)^{-1}\nabla Y_1$. This last relation is, however, merely an identity, because $Y_1 \equiv M_1 X_1/(M_1 X_1 + M_2 X_2)$ where M denotes the molecular weight, and $Y_1 + Y_2 \equiv 1 \equiv X_1 + X_2$, so that

$$\nabla Y_1 = M_1 M_2 \nabla X_1/(X_1 M_1 + X_2 M_2)^2.$$

The discussion of Spalding (1955) is not correct in this regard. For multicomponent diffusion the state of affairs is enormously more complicated. An excellent review of the problem is presented by Merk (1958) who shows that if diffusion coefficients are equal for all species, if the system is ideal (i.e. the activity coefficient of each species is unity), and if pressure and thermal diffusion are neglected, then the component mass fraction Y_i is a consistent variable for use as a 'driving force' in multicomponent situations. Presumably these results based upon application of irreversible thermodynamics apply with equal validity to turbulent flow.

Inspection of the energy equation (4) indicates the great simplification resulting from an assumption of unit value for Lewis number Le_T and Prandtl number Pr_T. Past experience indicates that the Lewis number equals unity even though neither the Schmidt number nor the Prandtl number may be individually equal to unity. In the low speed flow encountered here the dissipation term in the energy equation can be neglected even though $Pr_T \neq 1$. With $Le_T = 1$, the energy equation becomes:

$$\overline{\rho}\overline{u}\frac{\partial}{\partial x}(\overline{H} + \tfrac{1}{2}\overline{u}^2) + (\overline{\rho}\overline{v} + \overline{\rho' v'})\frac{\partial}{\partial y}(\overline{H} + \tfrac{1}{2}\overline{u}^2) = \frac{\partial}{\partial y}\left[\epsilon_\lambda \frac{\partial}{\partial y}\sum_i (\overline{h}_i \overline{Y}_i + \tfrac{1}{2}\overline{u}^2)\right]. \qquad (5)$$

It is quite important to observe that $\sum_i \overline{h}_i \overline{Y}_i \neq \overline{H}$ but rather, since $T \equiv \overline{T} + T'$ and $H \equiv \overline{H} + H'$ where

$$\overline{H} = \sum_i \overline{h}_i \overline{Y}_i + \sum_i \overline{h_i' Y_i'},$$

$$H' = \sum_i h_i' \overline{Y}_i + \sum_i Y_i' \overline{h}_i,$$

$$\overline{h}_i = \int_0^{\overline{T}} c_{p_i} dT + h_i^0,$$

$$h_i' = \int_{\overline{T}}^{\overline{T}+T'} c_{p_i} dT,$$

we have

$$\epsilon_\lambda \frac{\partial}{\partial y} \sum_i \bar{h}_i \bar{Y}_i = \epsilon_\lambda \frac{\partial \bar{H}}{\partial y} - \epsilon_\lambda \frac{\partial}{\partial y} \overline{h_i' Y_i'}.$$

In these expressions h_i^0 is the enthalpy of formation of component i, c_{p_i} its specific heat, and T the temperature. Previous treatments (Rose *et al.* 1958, for example) have overlooked the term in $\overline{h_i' Y_i'}$. In cases like the present situation where zones of intense reaction can occur the approximation $\partial \bar{H}/\partial y \gg \partial(\overline{h_i' Y_i'})/\partial y$ is perhaps a good one. Its validity everywhere in the flow field is an open question. For convenience we omit this term so that the energy equation takes the simple form (with $H_T \equiv \bar{H} + \frac{1}{2}\bar{u}^2$)

$$\bar{\rho}\bar{u} \frac{\partial H_T}{\partial x} + (\bar{\rho}\bar{v} + \overline{\rho' v'}) \frac{\partial H_T}{\partial y} = \frac{\partial}{\partial y} \left(\epsilon_\lambda \frac{\partial \bar{H}_T}{\partial y} \right). \tag{6}$$

The simplification of the species conservation equation is accomplished by rewriting it in terms of a particular *atomic* species, rather than a molecular species, in order to eliminate the troublesome source term W_i. Zeldovich (1951) was one of the first to make use of this technique. It is simplest to illustrate by introducing an atomic species coefficient $\beta_{j,i}$ representing the mass fraction of atomic species j in molecular compound i.

Thus if j were O_2 and i were CO_2 then $\beta_{j,i} = \frac{32}{44}$. Multiplying (3) by $\beta_{j,i}$ and summing on the index i we obtain, for equal diffusion coefficients, the useful form

$$\bar{\rho}\bar{u} \frac{\partial Y_j^*}{\partial x} + (\bar{\rho}\bar{v} + \overline{\rho' v'}) \frac{\partial Y_j^*}{\partial y} = \frac{\partial}{\partial y} \left(\rho \epsilon_d \frac{\partial Y_j^*}{\partial y} \right). \tag{7}$$

The term $Y_j^* \equiv \sum_i \beta_{j,i} Y_i$ is the mass fraction of atomic species j present in all chemical forms calculated from local composition measurements. The term $\sum_i \beta_{j,i} \bar{w}_i$ represents the net rate of production of atoms of species j which is equal to zero because atoms in a chemical reaction merely change their molecular associations and are not destroyed. Therefore a linear relationship between Y^* and H_T exists if appropriate boundary conditions can be satisfied. Specifically,

$$\frac{Y_j^* - Y_{j,w}^*}{Y_{j,e}^* - Y_{j,w}^*} = \frac{H_T - H_{T,w}}{H_{T,e} - H_{T,w}}. \tag{8}$$

The boundary condition for an element, like oxygen, which is not present in the fuel is

$$(\rho v)_w Y_{0,w}^* - \left(\rho \epsilon_d \frac{\partial Y_0^*}{\partial y} \right)_w = 0. \tag{9}$$

If the fuel is a pure hydrocarbon of α pounds of carbon per pound of fuel, the boundary condition written for the element carbon is

$$\alpha(\rho v)_w = (\rho v)_w Y_{c,w}^* - \left(\rho \epsilon_d \frac{\partial Y_c^*}{\partial y} \right). \tag{10}$$

Following Lees (1958) we can *arbitrarily* choose to define a Stanton number through the relationship

$$\left(\epsilon_\lambda \frac{\partial H_T}{\partial y} \right)_w \equiv \rho_e U_e St (H_{T,e} - H_{T,w}). \tag{11}$$

By noting that for $Le_T = 1$ we have $\epsilon_\lambda = \rho\epsilon_d$, and by defining a 'modified' blowing parameter $B' \equiv (\rho v)_w/\rho_e U_e St$, (9) can be written in the form

$$Y^*_{0,e}/Y^*_{0,w} = B' + 1. \tag{12}$$

Similarly (10), under the assumption $Y^*_{c,e} = 0$, becomes

$$Y^*_{c,w} = \alpha B'/B' + 1. \tag{13}$$

Evidently similar relationships hold for the other atomic species.

Wall energy balance

An energy balance on a section of porous wall, neglecting the detailed behaviour of the flow from the pores is

$$\left(\epsilon_\lambda \bar{c}_p \frac{\partial \overline{T}}{\partial y}\right)_{g,w} - \sum_i (\rho_i v_i h_i)_{g,w} + (\rho v)_w h_{injectant,\,solid} = \dot{q}_{solid} + \sigma\epsilon T^4_w. \tag{14}$$

The first two terms on the left represent energy transport from the gas by conduction and by diffusion or convection. The third term is the flow of energy into the wall-gas interface carried by the injectant. The two terms on the right represent heat conduction to the solid interior and radiation to the cool surroundings. In this equation $\bar{c}_p = \sum_i c_{p_i} Y_i$, σ is Boltzmann's constant, and ϵ is the emissivity of the porous wall. It is the nature of combustion chemistry that reactions essentially cease within some small, but finite distance from the wall. This means that for $i \neq I$, $\rho_i v_i \equiv 0$ so that $\rho_I v_I = (\rho v)_w$, where the subscript I refers to the injectant. Defining $\dot{q}_{wall} = \dot{q}_{solid} + \sigma\epsilon T^4_w$, the energy balance becomes simply

$$\left(\epsilon_\lambda \bar{c}_p \frac{\partial \overline{T}}{\partial y}\right) - (\rho v)_w L_I = \dot{q}_w, \tag{15}$$

where L_I is the heat of vaporization of the injectant. With $L_I = 0$ one obtains:

$$q_w = \left(\epsilon_\lambda \bar{c}_p \frac{\partial \overline{T}}{\partial y}\right)_{g,w}. \tag{16}$$

The important result is that wall heat transfer is due solely to conduction from the gas. Notice that the definition of Stanton number in terms of total enthalpy gradient does not yield the wall heat transfer directly. Rather, since

$$d\overline{H} = \bar{c}_p d\overline{T} + \sum_i \bar{h}_i d\overline{Y}_i + \tfrac{1}{2} d\bar{u}^2,$$

the wall heat transfer can be written as

$$q_w = \rho_e U_e St(H_{T,e} - H_{T,w}) - \rho\epsilon_d \sum_i \left(\bar{h}_i \frac{\partial \overline{Y}_i}{\partial y}\right)_w. \tag{17}$$

Furthermore, by multiplying the defining equation for species flux

$$\rho_i v_i = (\rho v)_w Y_i - \rho\epsilon_d \partial Y_i/\partial y$$

by h_i and summing over all species we obtain

$$\left(\rho\epsilon_d \sum_i \bar{h}_i \frac{\partial \overline{Y}_i}{\partial y}\right)_w = (\rho v)_w \sum_i \bar{h}_i \overline{Y}_i - (\rho v)_w \bar{h}_{I,w}. \tag{18}$$

With the aid of (18) and the definition of B' it is therefore possible to write (17) in the more useful form:

$$q_w = \rho_e U_e St[\sum_i \overline{Y}_{i,e}(\overline{h}_{i,e} - \overline{h}_{i,w}) + \sum_i \overline{h}_{i,w}(\overline{Y}_{i,e} - \overline{Y}_{i,w}) - B' \sum_{i \neq I} \overline{Y}_i \overline{h}_i - B' \overline{h}_{I,w}(Y_{I,w} - 1)]. \quad (19)$$

In the present case there is no injectant present in the main stream flow so that $Y_{I,e} = 0$. Equation (19) then takes a form previously derived by Lees (1958) and Bromberg & Lipkis (1958):

$$q_w = \rho_e U_e St\{\sum_i Y_{i,e}(h_{i,e} - h_{i,w}) + \sum_{i \neq I} h_{i,w}[Y_{i,e} - (B' + 1) Y_{O_2,w}]\}. \quad (20)$$

We now assume an overall one-step reaction for methane combustion:

$$CH_4 + 2O_2 \rightarrow CO_2 + 2H_2O.$$

Use of (12) and (13) together with the definition of heat of reaction per pound of oxygen

$$Q_{R,O_2,w} \equiv \tfrac{16}{64} h_{CH_4,w} + h_{O_2,w} - \tfrac{44}{64} h_{CO_2,w} - \tfrac{36}{64} h_{H_2O,w}$$

yields the form

$$q_w = (\rho v)_w (B')^{-1}\{\sum_i Y_{i,e}(h_{i,e} - h_{i,w}) + Q_{R,O_2,w}[Y_{O_2,e} - (B' + 1) Y_{O_2,w}]\}. \quad (21)$$

In the present work this expression was used to calculate B'. The other quantities were determined experimentally by composition and temperature measurements at the wall or from the known fuel-injection and free-stream flow rates. If there were no oxygen present at the wall, equation (21) would become

$$q_w = St\rho_e U_e[-Y_{O_2,e} h_{O_2,w} - Y_{N_2,e} h_{N_2,w} + Q_{R,O_2,w} Y_{O_2,e}], \quad (22)$$

showing that *only* in this case is the heat transfer explicitly independent of the blowing parameter B'.

Another instructive approximate form can be obtained if one takes the specific heats of O_2 and N_2 constant and equal at about 0·24 BTU/lb °F and, in addition, assumes that the specific heat of reactants is the same as that of products. It follows that the definition of adiabatic flame temperature can be put in the form

$$0{\cdot}24(T_{ad.f} - T_e) = \frac{0{\cdot}23 Q_{R,O_2,w}}{(1 + f/a)_{stoichiometric}},$$

where f/a is the fuel to air ratio, so that equation (22) becomes

$$q_w \approx St\rho_e U_e[(T_{ad.f} - T_w) + (f/a)_{stoichiometric}(T_{ad.f} - T_e)]. \quad (23)$$

Since, for most fuels, $(f/a)_{stoichiometric} \ll 1$ we obtain the final rough form:

$$q_w \approx St\rho_e U_e (c_p)_e (T_{ad.f} - T_w).$$

Therefore, we have reduced the reacting flow problem to a canonical form with $T_{ad.f}$ appearing as the driving force for heat transfer. This is similar to use of the recovery temperature in connexion with very-high-speed flow problems.

5. Experimental results

A. *Nature of the boundary layer without combustion*

Use of a hot wire probe within the boundary layer gave the turbulence profiles shown in figures 2 and 3*a*. These data show the percentage turbulence rising from a value of 4·5 % in the free stream to 11 % near the wall. A value of 7·8 % was obtained at the wall. The maximum value occurred at a distance from the wall corresponding to the location of the 'buffer zone' in the usual model of the flat-

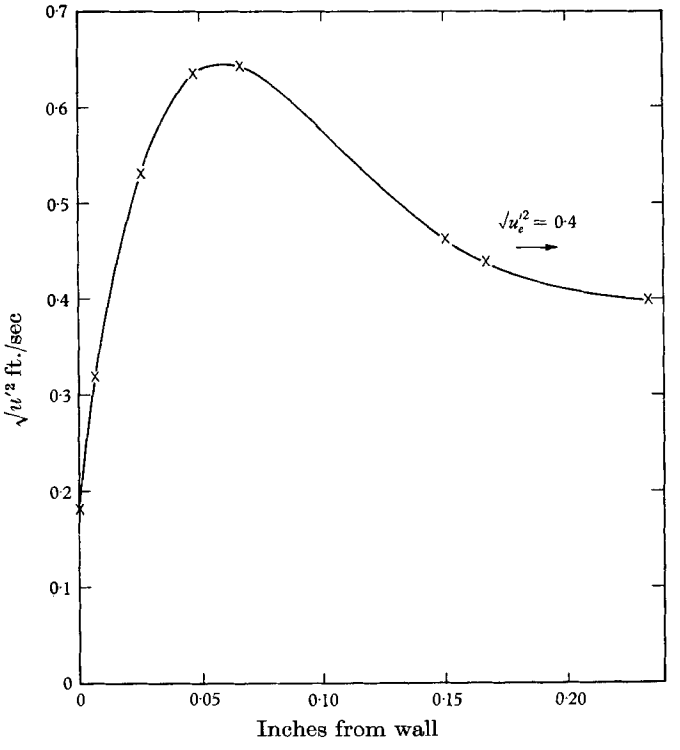

FIGURE 2. Typical distribution of turbulent fluctuating velocity component $\sqrt{u'^2}$ in boundary layer. $Re_x = 9 \times 10^4$; $x = 19{\cdot}5$ in.; $U_e = 9{\cdot}0$ ft./sec.

plate turbulent boundary layer. Additional evidence of the turbulent nature of the boundary layer was offered by the characteristic shape of velocity profiles obtained by means of pitot-tube traverses.

Injection of a fluid into the turbulent sublayer is likely to produce disturbances there and alter its usual laminar properties. Figure 3*b* shows results of traversing the boundary layer with the hot wire using air instead of the gaseous fuel as injectant. These results clearly show the increase in turbulent level attendant upon such injection.

B. *Mass transfer in the burning boundary layer*

In the present experiment, the magnitude of the mass transferred across the boundary layer was an independent variable controlled by the rate of fuel

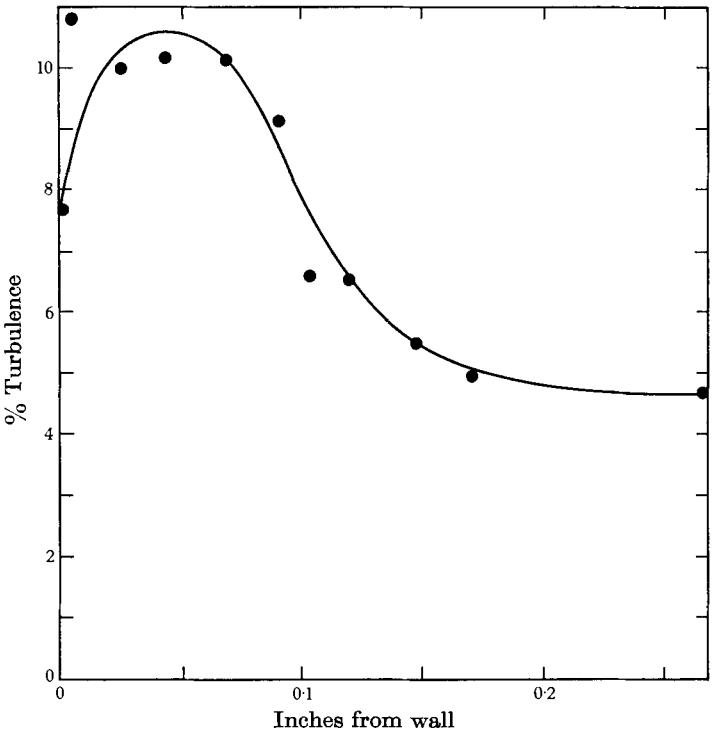

FIGURE 3*a*. Turbulence level (percentage) *vs.* distance from porous wall. % Turbulence level $\equiv \sqrt{u'^2}/u(y) \times 100$. $Re_x = 9 \times 10^4$; $x = 19{\cdot}5$ in.; $U_e = 9{\cdot}0$ ft./sec.

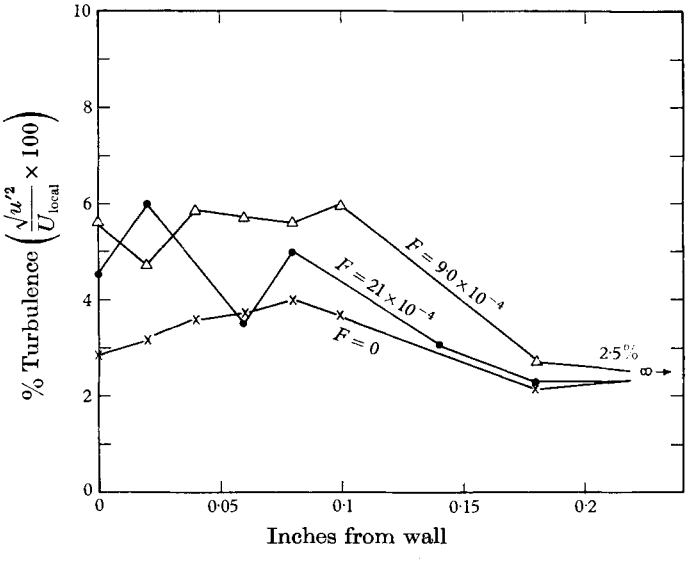

FIGURE 3*b*. Effect of mass injection on turbulence level. $F = (\rho v)_w/\rho_e U_e$; $Re = 4 \times 10^4$.

supplied. Therefore, the quantities of interest become the various species concentrations in the boundary layer. Typical composition profiles are shown in figures 4 to 6. These profiles were chosen because they illustrate the entire range of mole-fraction values encountered in the experiment. Composition is reported

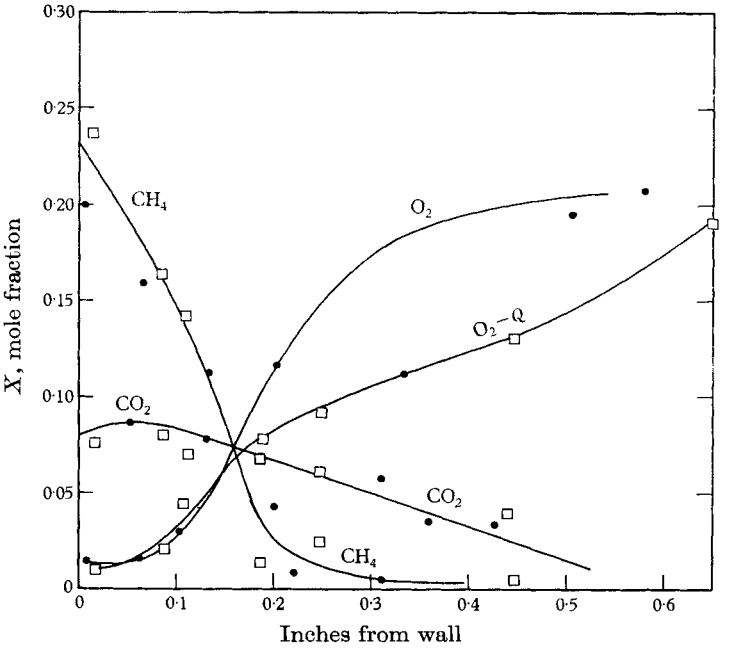

FIGURE 4. Species mole fraction distribution in burning boundary layer. $Re = 10^5$; $F = 0{\cdot}63 \times 10^{-3}$. ●, Stainless steel probe; □, quartz probe.

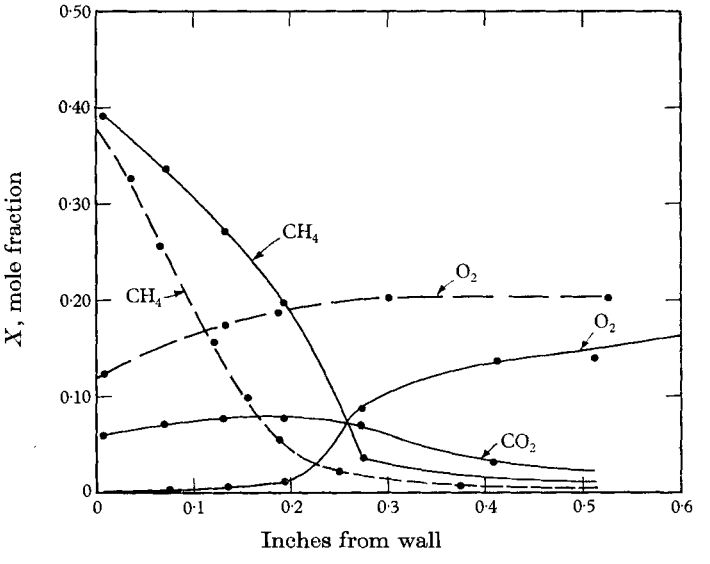

FIGURE 5. Species distribution in ignited and non-ignited boundary layer. $Re = 10^5$; $F = 1{\cdot}05 \times 10^{-3}$. ——, Injectant ignited; – – – –, injectant not ignited.

on a water-free basis. Four separate molecular compounds are identified: methane, carbon dioxide, oxygen and nitrogen. The amount of carbon monoxide was found to be less than 1 % in all cases.

It was necessary to determine whether chemical reactions occurred within the probe. If this were the case, measurements of composition would be in error in the sense of yielding incorrect values for the individual species. Atom ratios

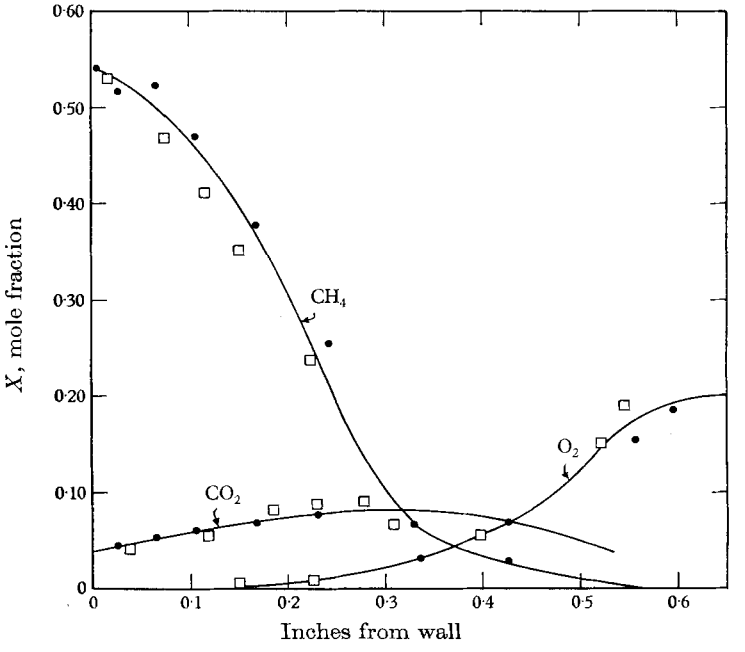

FIGURE 6. Species mole fraction distribution in burning boundary layer. $Re = 6{\cdot}3 \times 10^4$; $F = 1{\cdot}7 \times 10^{-3}$. ●, Stainless steel probe; □, quartz probe. $F \equiv (\rho v)_w/\rho_e U_e$.

like C/O or N/O would, of course, be unaltered by such reactions. Results of using quartz and stainless steel probes are indicated on figures 4 and 6. There is evidence of good agreement even though these materials possess vastly different catalytic properties.

Another interesting feature of the profiles is that the concentrations of oxygen and fuel are nowhere equal to zero. This suggests that the concept of a contact discontinuity between fuel and air is only a rough approximation to the real case.

As part of the theoretical discussion it was assumed that the diffusion coefficients of all species were identical. Therefore, the overall mass ratio of nitrogen to oxygen at most space points should be constant and equal to the measured value of 3·8 in the free stream, except near the wall where the effects of fuel injection are greatest. Experimental values of this ratio are plotted in figure 7, versus distance from the wall. The total amount of water actually present was computed by assuming the gas samples to have initially possessed a water content in stoichiometric proportion to the measured amount of carbon dioxide. The reasonableness of this assumption may be confirmed by reference to experiments of Gordon *et al.* (1958). As expected, most of the values are slightly above

3·8 and are about 10 % larger very near the porous wall. The example of the fuel injected, but not ignited, is seen not to differ appreciably from other hot flow results.

The injectant mass-transfer coefficient, defined by $k_G = (\tilde{\rho v})_w/(p_w - p_e)_{\text{fuel}}$, where p is the partial pressure, was calculated from the measured mass fuel fraction at the wall and in the free stream (the latter quantity being zero) together with the known rate of fuel injection. This coefficient was made dimension-

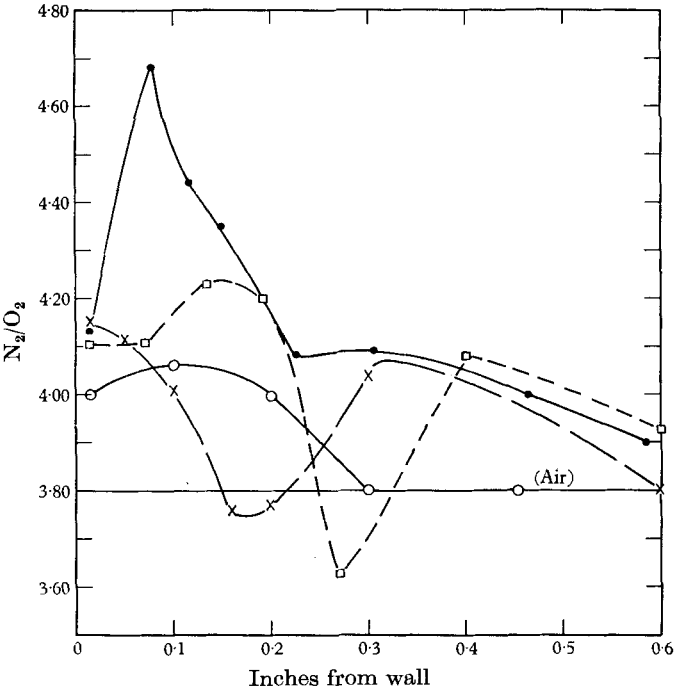

FIGURE 7. Ratio of nitrogen to total oxygen in burning boundary layer. The various curves are for the following conditions:

● $(\rho v)_w = 4{\cdot}6 \times 10^{-4}$, $Re = 10^5$, $F = 0{\cdot}63 \times 10^{-3}$;
× $(\rho v)_w = 7{\cdot}8 \times 10^{-4}$, $Re = 6{\cdot}3 \times 10^4$, $F = 1{\cdot}7 \times 10^{-3}$;
□ $(\rho v)_w = 7{\cdot}8 \times 10^{-4}$, $Re = 10^5$, $F = 1{\cdot}05 \times 10^{-3}$;
○ $(\rho v)_w = 7{\cdot}8 \times 10^{-4}$, $Re = 10^5$, $F = 1{\cdot}05 \times 10^{-3}$, fuel *not* ignited. $F \equiv (\rho v)_w/\rho_e U_e$.

less by incorporation into a standard form, analogous to the Stanton number for heat transfer,

$$j_D \equiv \frac{k_G M_e P}{\rho_e U_e} \frac{P_{BM}}{P} (Sc)^{\frac{2}{3}},$$

where M_e is the molecular weight in the free stream and P_{BM} is the logarithmic mean pressure ratio of all the other components evaluated at the wall and in the free stream. Figure 8 presents j_D plotted against a Reynolds number based on distance from the beginning of the porous wall and free stream properties. These data are presented in another form as figure 9, which plots the quantity F *vs* $\ln(1 - X_{CH_4})_w^{-1}$ with Reynolds number as a parameter. The expression for j_D is

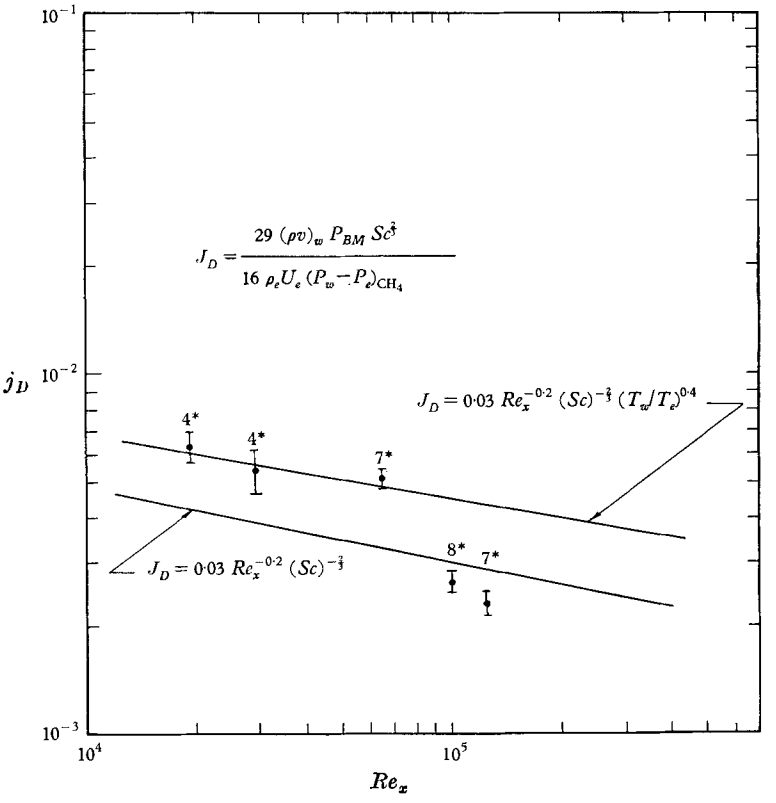

FIGURE 8. Mass-transfer coefficients with injection and combustion.
* Numerals refer to number of points in indicated range.

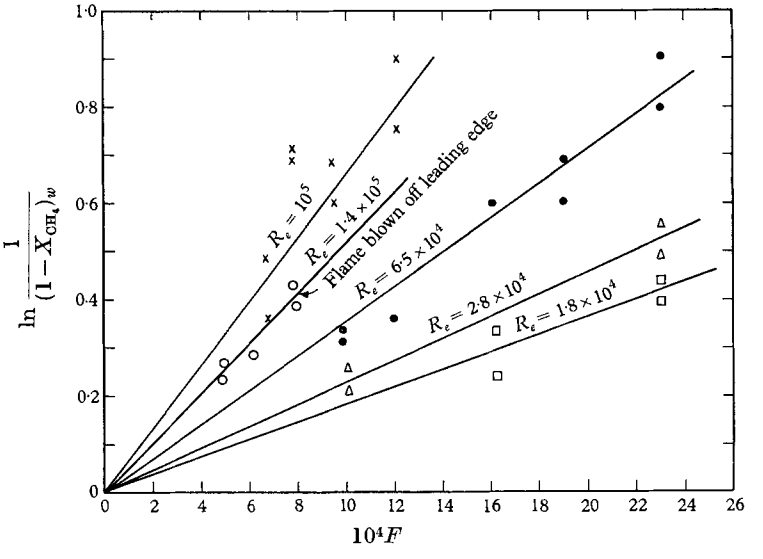

FIGURE 9. Correlation of wall composition measurements with injection rate; F *vs* $\ln (1 - X_{CH_4})_w^{-1}$. $F \equiv (\rho v)_w / \rho_e U_e$.

equivalent to $j_D \equiv M_e F(Sc)^{\frac{2}{3}}/M_I \ln(1-X_{CH_4})_w^{-1}$, where $F \equiv (\rho v)_w/\rho_e U_e$ and M_I is equal to 16. It is clear from the linear portion of the relationship between F and $\ln(1-X_{CH_4})_w^{-1}$ at fixed Re that j_D is a function of Reynolds number alone.

C. *Heat transfer in the burning boundary layer*

Typical temperature profiles determined with the chromel-alumel thermocouple are shown in figure 10. It was found that, for a given Reynolds number, the temperature distributions formed families of curves if plotted with fuel flow rate as parameter. The highest temperature recorded was 1640 °F. This figure

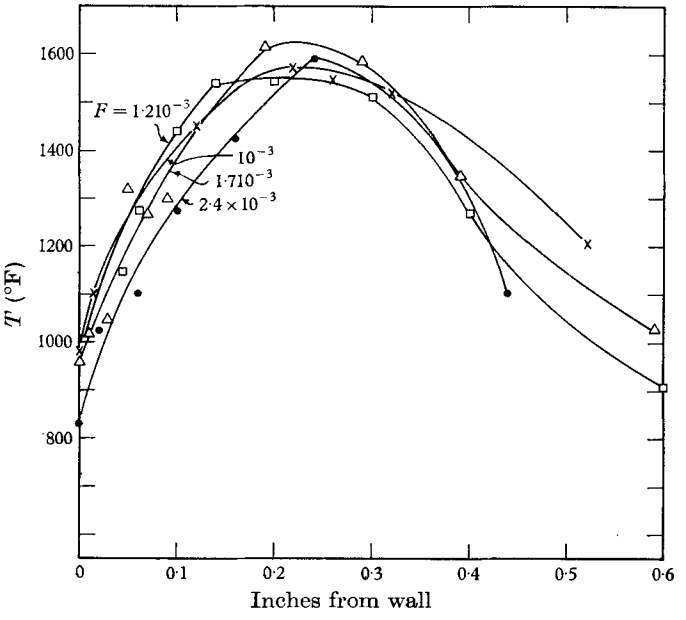

FIGURE 10. Temperature distribution for the burning boundary layer. Ambient temperature 75 °F, $Re = 6{\cdot}3 \times 10^4$. The various curves are
×, $F = 1{\cdot}0 \times 10^{-3}$; □, $F = 1{\cdot}2 \times 10^{-3}$; △, $F = 1{\cdot}7 \times 10^{-3}$; ●, $F = 2{\cdot}4 \times 10^{-3}$.
$F \equiv (\rho v)_w/\rho_e U_e$.

is below the adiabatic flame temperature for methane-air mixtures. However, the probe tip was of a thickness comparable to the reaction zone so that local quenching phenomena are probable. The situation was further complicated by small-scale turbulent fluctuations of the reaction zone so that a thermocouple will give an averaged value of local temperature.

In order to compute the Stanton number from (21) of the preceding section the net heat transfer to the porous wall was first calculated from experimental measurements. The radiation term $\dot{q}_r = \sigma\epsilon T_w^4$ was calculated using the measured wall temperature and an assumed value of $\epsilon = 0{\cdot}8$ for the slightly blacked, porous, metallic wall. Values of heat conduction through the porous tube walls were computed from measurements of energy removed by cooling water inside the tube plus the energy required to heat the fuel from its base temperature to the wall temperature. Fortunately, an independent check on the reported wall temperatures was available. Because the heat-transfer mechanism operating

inside the porous tube assembly was radiation from inside the porous wall it follows that $q_s \cong q_r$. This conclusion is contingent upon the assumptions of small temperature drop through the wall and emissivity of the inside wall being equal to that of the outside. The check on wall temperature values was provided by noting that q_r was indeed half the total heat transfer.

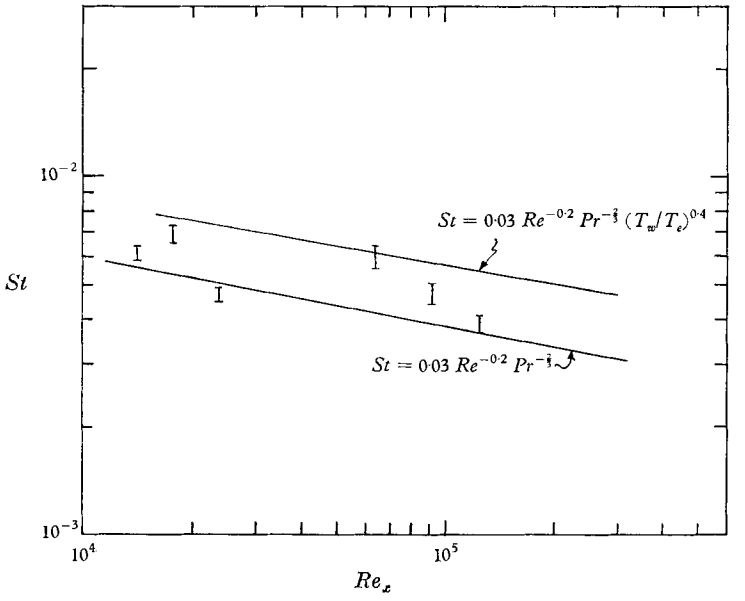

FIGURE 11. Stanton number based on theoretical enthalpy difference *vs* Reynolds number, where St is given by equation (21),

$$q_w = (\rho v)_w (B')^{-1} \{\sum_i Y_{i,e}(h_{i,e} - h_{i,w}) + Q_{R,O_2,w}[Y_{O_2,e} - (B'+1)Y_{O_2,w}]\}.$$

The Stanton numbers are plotted versus Reynolds number in figure 11. Also illustrated are various standard correlations for heat transfer to a solid wall with appreciable temperature variation through the boundary layer. Other definitions of St would lead to other placements of experimental points on figure 11.

D. *Momentum transfer in the burning boundary layer*

Shear stress to the wall was measured by means of a Stanton tube. The values were converted to a non-dimensional friction factor and plotted versus Reynolds number as shown in figure 12. Two correlating lines are drawn which indicate that the data can be grouped according to high or low values of the injection parameter B'.

Limits of validity of these measurements can be assessed by closer examination of the operation of the Stanton tube. The tube was calibrated, without the presence of mass injection, by first placing it against the porous wall. Next, free stream Reynolds number was varied and corresponding differences between total and static pressure, ΔP, were noted. These data were then plotted as $P = F(T)$ where

$$P \equiv \Delta P \rho_w h^2 g_c \mu_w^{-2}, \quad T = \tau_w \rho_w h^2 g_c.$$

The width of the probe, denoted by h, was constant and equal to 0·014 in.; g_c is 32·17 ft./sec^2 and μ_w is the value of viscosity at the wall. The wall shear stress τ_w was computed from the well-known flat-plate formula:

$$\tau_w = 0{\cdot}03 Re_x^{-0{\cdot}2} \rho_e U_e^2.$$

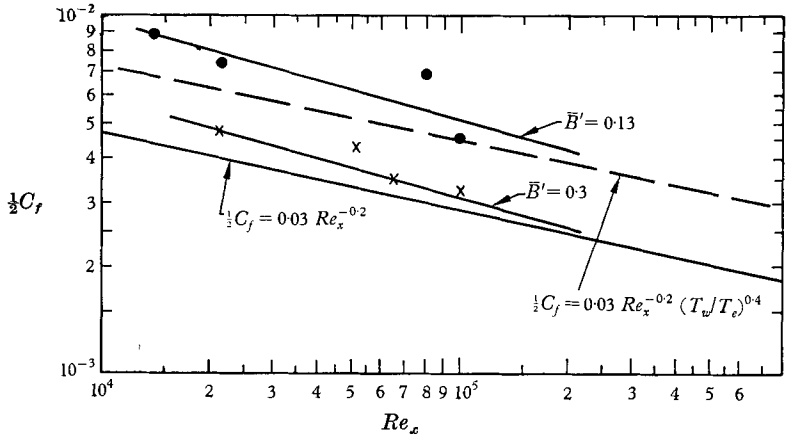

FIGURE 12. Skin-friction coefficient $\frac{1}{2}C_f$ *vs* Reynolds number with injection and combustion. $\bar{B}' = F/\frac{1}{2}C_f$. $F \equiv (\rho v)_w/\rho_e U_e$.

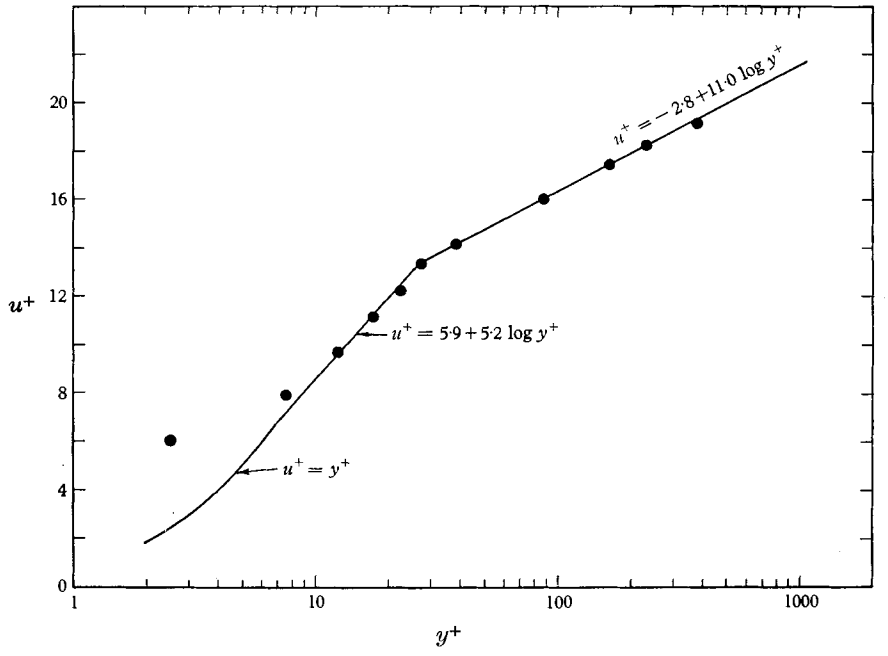

FIGURE 13. Dimensionless velocity distribution (no mass injection). $u^+ = u/(\tau_w/\rho)^{\frac{1}{2}}$, $y^+ = y(\tau_w/\rho)^{\frac{1}{2}}\rho/\mu$.

This choice of τ_w for use in the calibration formula was checked in the following manner. Velocity profiles were obtained in the boundary layer and the calculated value of shear stress was used to convert them to dimensionless u^+ versus y^+ form where $u^+ = u/(\tau_w/\rho)^{\frac{1}{2}}$ and $y^+ = y(\tau_w/\rho)^{\frac{1}{2}}\rho/\mu$. In this manner curves, such

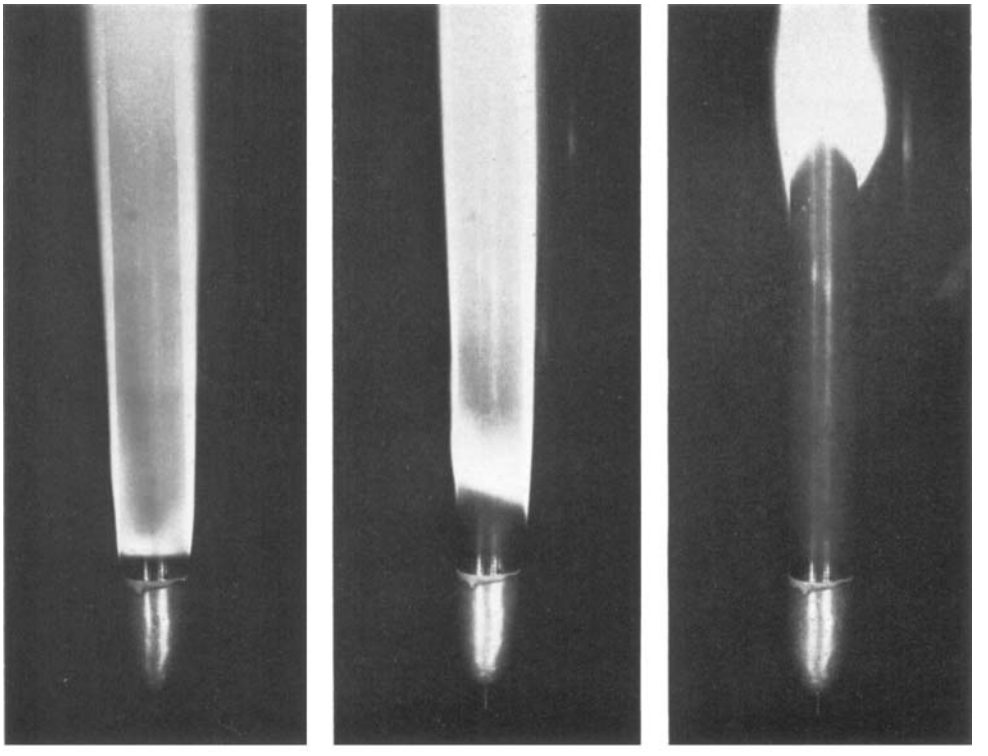

FIGURE 1*b* (plate 1). Flame stabilized at different positions along the tube.

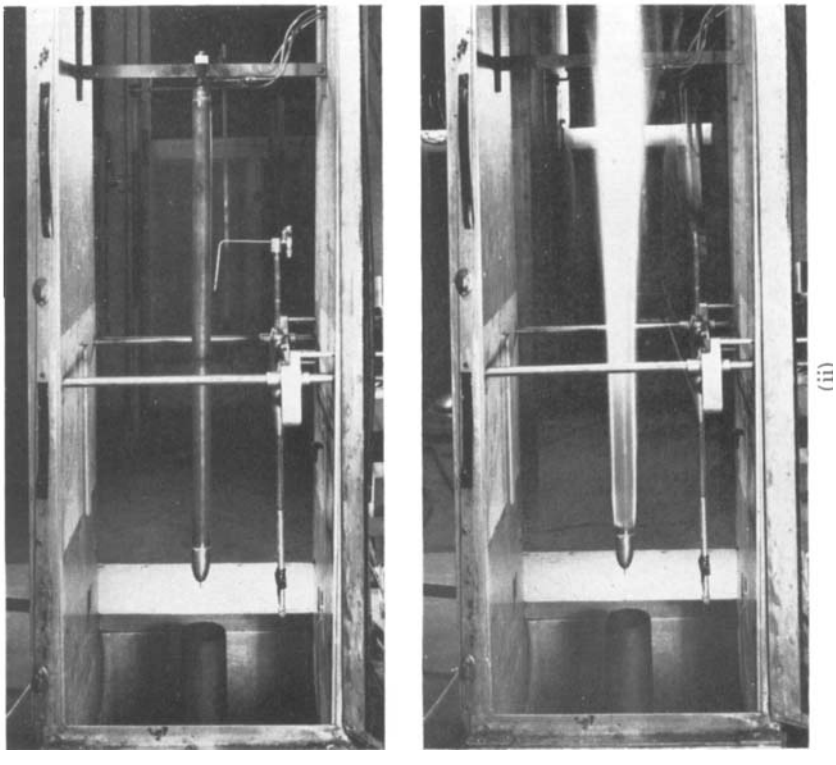

FIGURE 1*a* (plate 1). Tube mounted in wind tunnel: (i) no flow, (ii) gas ignited.

as the one shown in figure 13, were obtained. Agreement with usual results was quite good in the buffer layer and turbulent core régimes. The deviation from a linear relationship in the sublayer is an expected result in the vicinity of a roughened wall.

Use of the instrument in the presence of mass injection can only be partially justified. With regard to the calibration formula the effect of injection would be to drop values of τ_w by altering the velocity profiles near the wall. However, the Stanton tube cannot distinguish between changes in velocity profiles due to injection and those changes due to altered free-stream conditions if the profiles are similar. With the Stanton tube immersed in the sublayer of a turbulent boundary layer this condition takes the form of requiring the velocity to be linear with distance from the wall, even with mass injection. This will be true only for modest injection rates. Therefore the momentum transfer results must be regarded as tentative.

6. Discussion of results

Experimental values of the skin-friction coefficient, mass transfer number j_D, and Stanton number have been plotted versus Reynolds number in figure 14. The straight line drawn on this figure is given by the expression, transfer number $= 0{\cdot}038 Re_x^{-0{\cdot}2}$, and correlates heat and mass transfer results to within $\pm 30\,\%$. Friction factors at higher blowing rates ($B' \cong 0{\cdot}3$) are also correlated by this line. Reference to figure 12 shows that skin-friction coefficients corresponding to lower injection rates can be correlated by inclusion of a multiplicative term of the form $(T_w/T_e)^n$ in the expression for transfer number. Therefore, the three processes of heat, mass, and momentum transfer are analogous, even with combustion and injection in the boundary layer, because appropriate transfer coefficients, at the same Reynolds number, have approximately the same numerical values. We now examine the question of the specific effects of mass injection on each of the transport processes.

Considering skin friction, it appears that for sufficiently low injection rates momentum absorption at the wall by the injected fuel is small so that skin friction is only slightly lowered by this effect. However, ignition of this small amount of fuel results in substantial heat release, thereby affecting values of transport coefficients and hence the values of wall shear stress. At higher injection rates the resultant pronounced lowering of shear stress offsets the effects of elevated temperature.

The effect of fluid injection on values of Stanton number appears to be governed by two opposing phenomena. Injection lowers the wall temperature a small amount which results in a significant lowering of the energy radiated from the wall because of the fourth power dependence of radiation on temperature. At the same time, energy absorption by the fuel goes up linearly with fuel injection rate if the assumption is maintained that fuel leaves the porous wall at the wall temperature. Because these effects are opposite with regard to net energy transfer from gas to wall, the overall effect of mass injection on the Stanton number is small. For a given Reynolds number, figure 11 shows that data points corresponding to various injection rates lie within small ranges.

The situation with regard to effects of mass injection on the mass-transfer parameter is more subtle. In terms of experimental variables this quantity may be represented by the product of four dimensionless groups:

$$j_D \equiv \frac{(\rho v)_w}{\rho_e U_e X_w} \cdot \frac{M_e}{M_I} \cdot Sc^{\frac{2}{3}} \cdot \frac{P_{BM}}{P}.$$

The first two terms are strictly analogous to a Stanton number which is defined on the basis of energy transferred to the wall, namely, $C_h = q_w/\rho_e U_e \Delta H$. Therefore, in so far as the first three terms are concerned, the mass-transfer parameter will depend on injection rate together with values of gas composition at the wall and in the free stream, but not explicitly on composition *gradient* at the wall.

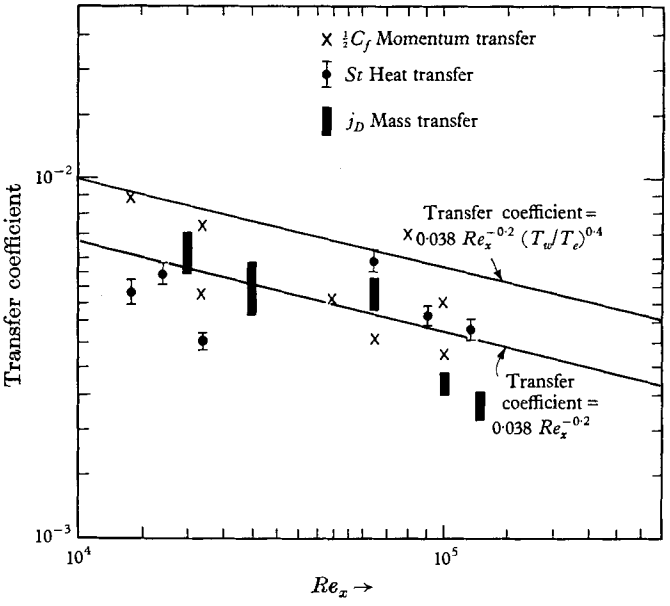

FIGURE 14. Dimensionless heat, mass, and momentum transfer coefficients *vs* Reynolds number.

Conversely, the definition of Stanton number used in the present work is based on the enthalpy gradient at the wall and not explicitly on the total amount of heat transferred, q_w. Of course, these quantities are related, as shown by equation (17). We now demonstrate that this difference is crucial insofar as determining variations of transfer coefficient with mass injection.

First, notice that the last term in the expression for j_D is the logarithmic mean pressure ratio of components in the gas mixture, excluding the injectant, based on free stream and wall conditions. This factor was first proposed as an empirical 'inert gas' correction by Colburn, as reported in Spalding (1955). He noted that for inert, small injection cases $j_D = C_h Pr^{\frac{2}{3}} = \frac{1}{2}C_f$ with C_h being defined in the manner of equation (11). It appears that this P_{BM}/P term occurs because of the non-zero mass fraction of the injectant at the wall and the resultant combination of both the convection and diffusion terms. To prove this we write equation (10)

for the injectant in terms of molar transport quantities and upon rearranging obtain

$$(\tilde{\rho}v)_I = \frac{\tilde{\rho}\mathscr{D}}{X_I - 1}\frac{dX_I}{dy}. \tag{a}$$

Integrating a short distance Δy into the stream, with $\rho\mathscr{D}$ assumed constant, yields:

$$(\tilde{\rho}v)_I = \tilde{\rho}\mathscr{D}\Delta_m^{-1}\frac{X_{I,w} - X_I}{\Delta y}, \tag{b}$$

where $$\Delta_m = \{X_{I,w} - X_I\}/\ln\{(X_{I,w} - 1)/(X_I - 1)\}.$$

The quantity Δm is equal to $-P_{BM}/P$ since static pressure is assumed constant across the boundary layer. Thus the amount of material transferred can be written as:

$$(\tilde{\rho}v)_I \simeq -\left(\tilde{\rho}\mathscr{D}\frac{P}{P_{BM}}\frac{\Delta X_I}{\Delta y}\right)_w. \tag{c}$$

Comparing this equation with the corresponding one for shear stress,

$$\tau_w \cong \left(\mu\frac{\Delta u}{\Delta y}\right)_w,$$

suggests that inclusion of the group P_{BM}/P with the dimensionless mass-transfer coefficient $kP/\rho_e U_e$ ought to give better numerical comparison with $\frac{1}{2}C_f$ or C_h. Therefore, it is not surprising that the effect of mass injection is not explicitly apparent in the mass-transfer results shown in figure 8 since, in fact, allowance has been made for this phenomena by means of the P_{BM}/P terms in the definition of j_D.

Experimentally it was found that the combustion zone did not significantly alter values of the gas composition near the wall relative to the inert injection case. Therefore, only the slope of the composition profiles at the wall will be affected by the boundary-layer reactions. Using the approximation $\rho D \propto T^{\frac{1}{2}}$ in equation (*a*) gives:

$$\left(\frac{\partial X_{\mathrm{CH_4}}}{\partial y}\right)_{w,\,\text{no combustion}} \cong \left(\frac{T_w}{T_e}\right)^{\frac{1}{2}}\left(\frac{\partial X_{\mathrm{CH_4}}}{\partial y}\right)_{w,\,\text{combustion}}$$

Reference to figure 5 shows the correctness of this relationship. Although the efficacy of transport processes in the boundary layer may be altered in the reacting situation, the requirements of the combustion processes act as a kind of boundary condition on possible values of fuel concentration and/or spacial gradient of this quantity within the boundary layer.

Although not presented in this paper, use of the 'rough' form for heat transfer $q_w = c_{pe}\rho_e U_e C_h(T_{ad.f} - T_w)$ gives a Stanton number which is somewhat above the upper line given on figure 11. Evidently, this sort of approximation is useful only when the wall concentration of oxygen is not known.

It is worth noting that the boundary-layer thicknesses based on distance from the wall required to effect 99 % recovery of free-stream values of temperature, velocity, or composition were very closely the same. This gives added support to the hypothesis of unit value for the Prandtl and Lewis number since it is known, at least in inert cases, that the ratio of thermal to velocity boundary-layer thickness, for example, is a simple power function of Prandtl number, viz. $\delta_T/\delta_u = (Pr)^{-\frac{1}{3}}$. The important result of these more detailed considerations is

that with the particular definitions of coefficients chosen in the present work, the presence of combustion plays a primary role in determining values of C_h and only a secondary role in determining values of j_D and $\frac{1}{2}C_f$. In addition, the effect of mass injection is primarily reflected by the values of $\frac{1}{2}C_f$ but not by C_h or j_D.

Conclusions

As a result of the present experimental investigation of co-existent heat, mass and momentum transfer processes within a combustible turbulent boundary layer where the fuel is injected through a porous wall it may be concluded that:

(1) For the range of fuel injection rates and Reynolds numbers encountered, the friction factor, mass transfer parameter, and Stanton number can be numerically correlated by an expression of the form $\frac{1}{2}C_f$, j_D, $St = 0{\cdot}038Re_x^{-0{\cdot}2}$ to within $\pm 30\,\%$ of measured values. Therefore, there exists a rough numerical analogy among all three processes.

(2) Values of the skin friction coefficient for low values of the blowing parameter $B' = (\rho v)_w/\rho_e U_e \frac{1}{2}C_f$ are reasonably well predicted by the ordinary flat plate formula

$$[\tfrac{1}{2}C_f]_{(\rho v)_w=0} = 0{\cdot}03Re_x^{-0{\cdot}2}\left(\frac{T_w}{T_e}\right)^{0{\cdot}4}.$$

If use is made of estimates of the known reduction in skin friction with mass injection then this simple correlation appears to be valid for predicting $\frac{1}{2}C_f$ at higher values of B'.

(3) The effect of mass injection on values of the Stanton number cannot be assessed with certainty as a result of an assumption that the injected fuel leaves the wall at wall temperature. If this surmise is correct then the Stanton number is substantially a constant with respect to changes in fuel injection rate.

(4) There is no effect of mass injection on the mass transfer number, j_D. This finding was shown to be an implicit result of the definition of j_D.

(5) The above facts indicate that an analogy among the three transport processes exists only within numerical limits and not in detail with respect to the influence of other parameters.

(6) The presence of the reaction zone has no unusual or special effects on boundary-layer transport phenomena other than the implicit effect of elevated temperature on values of transport and thermodynamic properties. Thus, there was no evidence for any sort of reaction generated turbulence.

(7) A stable turbulent diffusion flame with fuel injected through a porous wall may be established within a turbulent boundary layer without the use of a flame holder. The stabilizing mechanism is believed to be the presence of a preheated boundary layer on the $3\frac{3}{4}$ in. brass nose preceding the start of the porous cylinder.

This paper is based upon a doctoral thesis presented by the author to the Division of Engineering and Applied Physics, Harvard University, June 1960. Support was provided by the Office of Ordnance Research, U.S. Army, under contract nos. DA–19–020–ORD–1029 and DA–19–020–ORD–4609.

REFERENCES

BROMBERG, R. & LIPKIS, R. P. 1958 Heat transfer in boundary layers with chemical reactions due to mass addition. *Jet Propulsion*, **28**, 659.

GORDON, A. S. *et al.* 1958 Study of the chemistry of diffusion flames. *Seventh (International) Symposium on Combustion.* London: Butterworths Scientific Publications.

LEES, L. 1958 Convective heat transfer. Article in *Combustion and propulsion, 3rd Agard Symposium*, p. 451. New York: Pergamon Press.

MERK, H. J. 1958 The macroscopic equations for simultaneous heat and mass transfer in isotropic, continuous and closed systems. *Appl. Sci. Res.* A, **8**, 73.

PRESTON, J. H. 1959 The determination of turbulent skin friction by means of pitot tubes. *J. Roy. Aero. Soc.* **58**, 109–21.

ROSE, P. H. *et al.* 1958 Turbulent heat transfer on highly cooled blunt nosed bodies of revolution in dissociated air. *Heat Transfer and Fluid Mechanics Institute Proceedings.* Stanford.

SPALDING, D. B. 1955 *Some Fundamentals of Combustion*, p. 54. New York: Academic Press.

ZELDOVICH, Y. B. 1951 On the theory of combustion of initially unmixed gases. *Nat. Adv. Comm. Aero., Wash., Tech. Mem.* no. 1296.